9212 *Inorg. Chem.* **2010**, *49*, 9212–9216
DOI: 10.1021/ic1006742

Inorganic Chemistry
Article

$BaGa_4Se_7$: A New Congruent-Melting IR Nonlinear Optical Material

Jiyong Yao,[†,‡] Dajiang Mei,[†,‡,§] Lei Bai,[†,‡] Zheshuai Lin,[†,‡] Wenlong Yin,[†,‡,§] Peizhen Fu,[†,‡] and Yicheng Wu*[,†,‡]

[†]*Center for Crystal Research and Development, Technical Institute of Physics and Chemistry, Chinese Academy of Sciences, Beijing 100190, P.R. China,* [‡]*Key Laboratory of Functional Crystals and Laser Technology, Chinese Academy of Sciences, Beijing 100190, P.R. China, and* [§]*Graduate University of Chinese Academy of Sciences, Beijing 100049, P.R. China*

Received April 12, 2010

The new compound $BaGa_4Se_7$ has been synthesized for the first time. It crystallizes in the monoclinic space group *Pc* with $a = 7.6252$ (15) Å, $b = 6.5114$ (13) Å, $c = 14.702$ (4) Å, $\beta = 121.24$ (2)°, and $Z = 2$. In the structure, $GaSe_4$ tetrahedra share corners to form a three-dimensional framework with cavities occupied by Ba^{2+} cations. The material is a wide-band gap semiconductor with the visible and IR optical absorption edges being 0.47 and 18.0 μm, respectively. $BaGa_4Se_7$ melts congruently at 968 °C and exhibits a second harmonic generation response at 1 μm that is approximately 2−3 times that of the benchmark material $AgGaS_2$. A first-principles calculation of the electronic structure, linear and nonlinear optical properties of $BaGa_4Se_7$ was performed. The calculated birefractive index $\Delta n = 0.08$ at 1 μm and the major SHG tensor elements are: $d_{11} = 18.2$ pm/V and $d_{13} = -20.6$ pm/V. This new material is a very promising NLO crystal for practical application in the IR region.

Introduction

Nonlinear optical (NLO) materials have important applications in laser frequency conversion, optical parameter oscillator (OPO), and signal communication.[1] According to the application wavelength ranges, NLO crystals can be divided into three main groups, which are ultraviolet (UV) NLO crystals, visible NLO crystals, and infrared (IR) NLO crystals. In the past decades, several NLO crystals which have largely satisfied the practical requirements in the UV and visible regions have been found, such as $KTiOPO_4$ (KTP),[2] $LiNbO_3$,[3] β-BaB_2O_4 (BBO),[4] and LiB_3O_5 (LBO).[5] For IR NLO crystals, most of those in practical use belong to the ABC_2 chalcopyrite structure type, including $AgGaQ_2$ (Q = S, Se)[6,7] and $ZnGeP_2$.[8] These chalcopyrite type crystals possess advantages including large NLO coefficients and wide transparent regions in the IR region. However, they also have shortcomings of one kind or another which has seriously limited their applications. For example, $AgGaQ_2$ (Q = S, Se) has a low laser damage threshold, whereas $ZnGeP_2$ exhibits two-photon absorption of 1 μm laser (Nd:YAG).[9] Thus the search for new IR NLO crystals has become one of the key research areas in NLO materials chemistry.[10−12]

The search for new IR NLO materials includes investigating the NLO properties of existing noncentrosymmetric (NCS) structures and synthesizing new compounds with NLO properties, in the hope of discovering a new IR NLO material with better overall properties than the current materials and realizing a breakthrough in IR NLO crystal research. With effort, many new metal chalcogenides and metal halides with attractive NLO properties have been synthesized.[13−17] For example, the $AZrPSe_6$ (A = K, Rb, Cs) series of compounds[13] and $Cs_5BiP_4Se_{12}$[14] possess very

*To whom correspondence should be addressed. E-mail: ycwu@mail.ipc.ac.cn.

(1) Burland, D. M.; Miller, R. D.; Walsh, C. A. *Chem. Rev.* **1994**, *94*, 31–75.
(2) Driscoll, T. A.; Hoffman, H. J.; Stone, R. E.; Perkins, P. E. *J. Opt. Soc. Am. B* **1986**, *3*, 683–686.
(3) Boyd, G. D.; Miller, R. C.; Nassau, K.; Bond, W. L.; Savage, A. *Appl. Phys. Lett.* **1964**, *5*, 234–236.
(4) Chen, C.; Wu, B.; Jiang, A.; You, G. *Sci. Sin. B* **1985**, *28*, 235–243.
(5) Chen, C.; Wu, Y.; Jiang, A.; Wu, B.; You, G.; Li, R.; Lin, S. *J. Opt. Soc. Am. B* **1989**, *6*, 616–621.
(6) Chemla, D. S.; Kupecek, P. J.; Robertson, D. S.; Smith, R. C. *Opt. Commun.* **1971**, *3*, 29–31.
(7) Boyd, G. D.; Kasper, H. M.; McFee, J. H.; Storz, F. G. *IEEE J. Quantum Electron.* **1972**, *8*, 900–908.
(8) Boyd, G. D.; Buehler, E.; Storz, F. G. *Appl. Phys. Lett.* **1971**, *18*, 301–304.
(9) Schunemann, P. G. *AIP Conf. Proc.* **2007**, *916*, 541–559.
(10) Zawilski, K. T.; Schunemann, P. G.; Setzler, S. D.; Pollak, T. M. *J. Cryst. Growth.* **2008**, *310*, 1891–1896.
(11) Wu, H.; Cheng, G.; Yang, L.; Mao, M. *J. Synth. Cryst.* **2003**, *32*, 13–15.
(12) Isaenko, L.; Vasilyeva, I.; Merkulov, A.; Yelisseyev, A.; Lobanov, S. *J. Cryst. Growth* **2005**, *275*, 217–223.
(13) Banerjee, S.; Malliakas, C. D.; Jang, J. I.; Ketterson, J. B.; Kanatzidis, M. G. *J. Am. Chem. Soc.* **2008**, *130*, 12270–12272.
(14) Chung, I.; Song, J. H.; Jang, J. I.; Freeman, A. J.; Ketterson, J. B.; Kanatzidis, M. G. *J. Am. Chem. Soc.* **2009**, *131*, 2647–2656.
(15) Zhang, G.; Qin, J.; Liu, T.; Li, Y.; Wu, Y.; Chen, C. *Appl. Phys. Lett.* **2009**, *95*, 261104−1–261104−3.
(16) Guo, S. P.; Guo, G. C.; Wang, M. S.; Zou, J. P.; Xu, G.; Wang, G. J.; Long, X. F.; Huang, J. S. *Inorg. Chem.* **2009**, *48*, 7059–7065.
(17) Kim, Y.; Seo, I. S.; Martin, S. W.; Baek, J.; Halasyamani, P. S.; Arumugam, N.; Steinfink, H. *Chem. Mater.* **2008**, *20*, 6048–6052.

 Published on Web 09/23/2010

large second-harmonic generation (SHG) effects, whereas Na_3SbF_6 exhibits a very high laser damage threshold.[15] Another recent example is $BaGa_4S_7$. The crystal structure of $BaGa_4S_7$ was reported in 1983[18] and its melting point was reported in 2005.[19] In 2009, it was found to be an IR NLO material with NLO effect close to that of $LiGaS_2$.[20] In $BaGa_4S_7$, the microscopic functional group of NLO property is the GaS_4 tetrahedra, just as in the chalcopyrite type IR NLO materials such as $AGaQ_2$ (A = Li, Ag; Q = S, Se).[21,22]

We examined the structure of $BaGa_4S_7$ in detail and found that Ba is coordinated to a "loose" polyhedron of twelve S atoms with the shortest Ba−S bond being 3.40(2) Å,[18] which is 0.2 Å longer than the common Ba−S bond length. In other words, there may be other "more stable" structures with closer and stronger cation−anion interactions in the A/M/Q (A = alkaline-earth metal; M = In, Ga; Q = S, Se, Te) system. Thus we carried out a systematic exploratory investigation in the A/M/Q (A = alkaline-earth metal; M = In, Ga; Q = S, Se, Te) system in order to find new NCS structures consisting of MQ_4 tetrahedral building blocks and thus probably exhibiting NLO property, which has led to the discovery of $BaGa_4Se_7$, a new compound that crystallizes in the monoclinic space group *Pc*. In this paper, we report the synthesis, crystal structure, linear and nonlinear optical properties, and theoretical calculation on $BaGa_4Se_7$. This material shows a large SHG effect approximately 2−3 times that of the benchmark material $AgGaS_2$ when probed at Nd:YAG 1.064 μm laser pumping. Furthermore, it shows congruent-melting behavior, a property that is of great importance for the crystal growth and further practical application of chalcogenide NLO materials.

Experimental Section

Solid-State Synthesis. The following reagents were used as obtained: Ba (98+%), Se (99%), Ga (99%). Binary BaSe and Ga_2Se_3 were synthesized by the stoichiometric reactions of elements at high temperatures in sealed silica tubes evacuated to 1×10^{-3} Pa. Polycrystalline samples of $BaGa_4Se_7$ were synthesized by solid-state reaction techniques. A mixture of BaSe and Ga_2Se_3 in the molar ratio of 1:2 was grounded and loaded into a fused-silica tube under an Ar atmosphere in a glovebox. The tube was sealed under a 1×10^{-3} Pa atmosphere and then placed in a computer-controlled furnace. The sample was heated to 900 °C in 20 h and kept at that temperature for 72 h, and the furnace was then turned off.

X-ray powder diffraction analysis of the resultant powder sample was performed at room temperature in the angular range of $2\theta = 10-70°$ with a scan step width of 0.02° and a fixed counting time of 1 s/step using an automated Bruker D8 X-ray diffractometer equipped with a diffracted monochromator set for Cu K_α (λ = 1.5418 Å) radiation. The experimental powder X-ray diffraction pattern did not match any pattern in the database and was later found to be in agreement with the calculated pattern on the basis of the single-crystal crystallographic data of $BaGa_4Se_7$ (Figure 1).

Single-Crystal Growth. The as-prepared $BaGa_4Se_7$ powder was loaded into a fused-silica tube under an Ar atmosphere in a glovebox. The tube was sealed under a 1×10^{-3} Pa atmosphere and then placed in a computer-controlled furnace. The sample was heated to 1050 °C in 20 h, kept at that temperature for 72 h, and cooled at 2 K/h to 700 °C; the furnace was then turned off. The product consisted of yellow crystals of $BaGa_4Se_7$ in millimeter size. Analysis of the crystal with an EDX-equipped Hitachi S-3500 SEM showed the presence of Ba, Ga, and Se in the approximate molar ratio of 1:4:7. The crystal is stable in air.

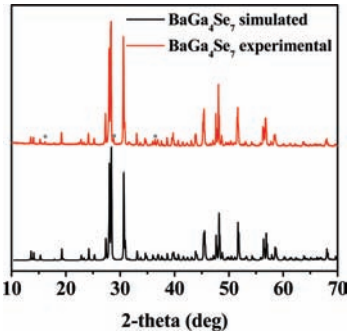

Figure 1. Experimental (top) and simulated (bottom) X-ray powder diffraction data of $BaGa_4Se_7$ (The three peaks marked with * are due to very small amount of $BaGa_2Se_4$, which crystallizes in the centrosymmetric space group *Cccm*).

Table 1. Crystal Data and Structure Refinements for $BaGa_4Se_7$

	$BaGa_4Se_7$
fw	968.94
T (°C)	−180
a (Å)	7.6252 (15)
b (Å)	6.5114 (13)
c (Å)	14.702 (4)
β (deg)	121.24(2)
V (Å^3)	624.1 (2)
space group	*Pc*
Z	2
ρ_c (g/cm^3)	5.156
μ (cm^{-1})	319.9
$R(F)^a$	0.0275
$R_w(F_o^2)^b$	0.0532

$^a R(F) = \Sigma||F_o| - |F_c||/\Sigma|F_o|$ for $F_o^2 > 2\sigma(F_o^2)$. $^b R_w(F_o^2) = \{\Sigma [w(F_o^2 - F_c^2)^2]/\Sigma wF_o^4\}^{1/2}$ for all data. $w^{-1} = \sigma^2(F_o^2) + (z\,P)^2$, where $P = (\mathrm{Max}(F_o^2, 0) + 2\,F_c^2)/3$; $z = 0.009$.

Structure Determination. Single-crystal X-ray diffraction data were collected with the use of graphite-monochromatized Mo K_α radiation (λ = 0.71073 Å) at −180 °C on a Rigaku AFC10 diffractometer equipped with a Saturn CCD detector. Crystal decay was monitored by recollecting 50 initial frames at the end of data collection. The collection of the intensity data was carried out with the program Crystalclear.[23] Cell refinement and data reduction were carried out with the use of the program Crystalclear,[23] and face-indexed absorption corrections were performed numerically with the use of the program XPREP.[24]

The structure was solved with the direct methods program SHELXS and refined with the least-squares program SHELXL of the SHELXTL.PC suite of programs.[24] The final refinement included anisotropic displacement parameters and a secondary extinction correction. The crystal was a racemic merohedral twin with fractional contributions of domains being 0.53, 0.39, 0.05, and 0.03. The program STRUCTURE TIDY[25] was then employed to standardize the atomic coordinates. Additional experimental details are given in Table 1 and selected metrical data are given in Table 2. Further information may be found in the Supporting Information.

Diffuse Reflectance Spectroscopy. A Cary 5000 UV−visible−NIR spectrophotometer with a diffuse reflectance accessory was

(18) Eisenmann, B.; Jakowski, M.; Schaefer, H. *Rev. Chim. Miner.* **1983**, *20*, 329–337.
(19) Hidaka, C.; Goto, M.; Kubo, M.; Takizawa, T. *J. Cryst. Growth.* **2005**, *275*, e439–e443.
(20) Lin, X.; Zhang, G.; Ye, N. *Cryst. Growth. Des.* **2009**, *9*, 1186–1189.
(21) Bai, L.; Lin, Z. S.; Wang, Z. Z.; Chen, C. T. *J. Appl. Phys.* **2008**, *103*, 083111/1–083111/6.
(22) Bai, L.; Lin, Z. S.; Wang, Z. Z.; Chen, C. T.; Lee, M.-H. *J. Chem. Phys.* **2004**, *120*, 8772–8778.
(23) *CrystalClear*; Rigaku Corporation: Tokyo, 2008.
(24) Sheldrick, G. M. *Acta Crystallogr., Sect. A* **2008**, *64*, 112–122.
(25) Gelato, L. M.; Parthé, E. *J. Appl. Crystallogr.* **1987**, *20*, 139–143.

Table 2. Selected Bond Lengths (Å) for $BaGa_4Se_7$

$BaGa_4Se_7$		$BaGa_4Se_7$	
Ba−Se1	3.6106(19)	Ga2−Se1	2.401(3)
Ba−Se1	3.659(2)	Ga2−Se2	2.382(2)
Ba−Se2	3.429(2)	Ga2−Se3	2.373(3)
Ba−Se3	3.4952(18)	Ga2−Se7	2.478(2)
Ba−Se4	3.834(2)	Ga3−Se3	2.363(3)
Ba−Se5	3.482(3)	Ga3−Se4	2.421(3)
Ba−Se6	3.541(3)	Ga3−Se6	2.361(2)
Ba−Se7	3.861(2)	Ga3−Se7	2.451(3)
Ga1−Se1	2.378(3)	Ga4−Se2	2.368(3)
Ga1−Se4	2.432(3)	Ga4−Se4	2.488(2)
Ga1−Se5	2.363(2)	Ga4−Se5	2.390(3)
Ga1−Se7	2.451(3)	Ga4−Se6	2.386(3)

used to measure the spectrum of $BaGa_4Se_7$ over the range of 200 nm (6.25 eV) to 2500 nm (0.50 eV).

Middle IR Transmission Spectroscopy. The middle IR transmission spectrum was measured with the use of a VERTEX 80 V FTIR spectrometer in the range of 250−4000 cm^{-1} on a 1 mm thick crystal at room temperature. The spectrum resolution is 2 cm^{-1}.

Thermal Analysis. The thermal property was investigated by the differential scanning calorimetric (DSC) analysis using the Labsys TG-DTA16 (SETARAM) thermal analyzer (the DSC was calibrated with Al_2O_3). About 60 mg of $BaGa_4Se_7$ was used for the DSC measurement. The $BaGa_4Se_7$ sample was placed in an Al_2O_3 crucible with surrounding N_2 gas at a rate of 60 mL/min to avoid the oxidation of $BaGa_4Se_7$ at elevated temperatures. The heating rate was 10 °C/min.

Second-Harmonic Generation Measurement. An optical second-harmonic generation (SHG) test was performed on the powder sample of $BaGa_4Se_7$ by means of the Kurtz−Perry method.[26] Fundamental 1064 nm light was generated with a Q-switched Nd:YAG laser. The particle size of the sieved sample is 80−100 μm. Microcrystalline $AgGaS_2$ of similar particle size served as a reference.

Theoretical Calculation. The electronic property calculations were performed using the first principles plane-wave pseudopotential method[27] implemented in the CASTEP package.[28] Normal-conserving pseudopotentials[29,30] are chosen and the valence electrons are 4s, 4p for selenium; 3d, 4s, 4p electrons for gallium; and 5s, 5p, 5d, 6s electrons for barium. Local-density approximation (LDA) with a very high kinetic energy cutoff of 900 eV is adopted. Monkhorst−Pack[31] k point meshes with a density of (4 × 4 × 2) points in the Brillouin zone of the unit cell are used.

Results and Discussion

Structure. $BaGa_4Se_7$ crystallizes in space group Pc of the monoclinic system. In the asymmetric unit, there is one crystallographically unique Ba atom, four unique Ga atoms, and seven unique Se atoms. The Ba atoms are coordinated to a bicapped trigonal prism of eight Se atoms, the Ga atoms are coordinated to a tetrahedron of four Se atom. Because there are no Se−Se bonds in the structures, the oxidation states of 2+, 3+, and 2− can be assigned to Ba, Ga, and Se, respectively.

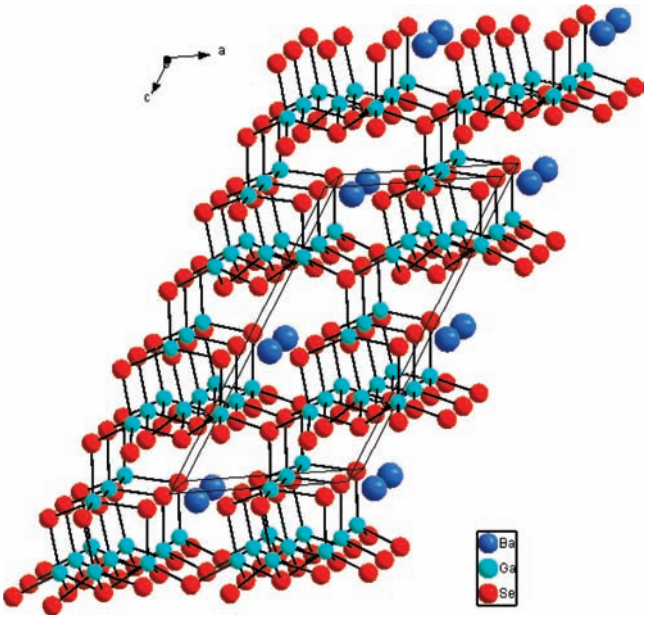

Figure 2. Structure of the $BaGa_4Se_7$ structure viewed along [010].

The structure of $BaGa_4Se_7$ is illustrated in Figure 2. The $GaSe_4$ tetrahedra are connected to each other by corner-sharing to form a three-dimensional framework with Ba cation in the cavities. Each Ba atom is coordinated to a bicapped trigonal prism of eight Se atoms. The Ba−Se bond lengths (Table 2) range from 3.429(2) to 3.861(2) Å, comparable to those of 3.212 (2)−3.873(2) Å in $Ba_2In_2Se_5$.[32] The Ga−Se bond lengths range from 2.361(2) to 2.488(2) Å, consistent with that of 2.443 (1) Å in $AgGaSe_2$.[33]

Of all the compounds reported in the A/M/Q system (A = alkaline-earth; M = In, Ga; Q = S, Se, Te), only two compounds crystallize as three-dimensional anionic framework, namely $CaGa_6Te_{10}$[34,35] and $BaGa_4S_7$.[18,20] $CaGa_6Te_{10}$ crystallizes in the space group $R32$ and in the structure $GaTe_4$ tetrahedra share both corners and edges to former a three-dimensional framework with cavities occupied by Ca^{2+} cations.[34,35] For $BaGa_4S_7$, the three-dimensional anionic framework is formed by corner-sharing GaS_4 tetrahedra only, as in the case of $BaGa_4Se_7$.

Although $BaGa_4Se_7$ possesses the same stoichiometry as $BaGa_4S_7$, the two crystallize in different space groups (Pc vs $Pmn2_1$). Their structures have some similarities: in both, the GaQ_4 tetrahedra (Q = S, Se) share corners to form a three-dimensional framework. However, the GaQ_4 tetrahedra is a bit more distorted in $BaGa_4Se_7$ than in $BaGa_4S_7$, because the largest difference between the Ga−Q bond lengths within a GaQ_4 tetrahedron is 0.118(2) Å for $BaGa_4Se_7$ and 0.088 (2) Å for $BaGa_4S_7$. Another obvious difference between these two structures is the coordination environment of Ba. In $BaGa_4S_7$, the Ba atom is coordinated to twelve S atoms with the shortest Ba−S distance being 3.400(2) A,[18] whereas in $BaGa_4Se_7$, the Ba is more " tightly" surrounded by eight Se atoms with the

(26) Kurtz, S. K.; Perry, T. T. *J. Appl. Phys.* **1968**, *39*, 3798–3813.
(27) Payne, M. C.; Teter, M. P.; Allan, D. C.; Arias, T. A.; Joannopoulos, J. D. *Rev. Mod. Phys.* **1992**, *64*, 1045–1097.
(28) Clark, S. J.; Segall, M. D.; Pickard, C. J.; Hasnip, P. J.; Probert, M. J.; Refson, K.; Payne, M. C. *Z. Kristallogr.* **2005**, *220*, 567–570.
(29) Rappe, A. M.; Rabe, K. M.; Kaxiras, E.; Joannopoulos, J. D. *Phys. Rev. B* **1990**, *41*, 1227–1230.
(30) Lin, J. S.; Qtseish, A.; Payne, M. C.; Heine, V. *Phys. Rev. B* **1993**, *47*, 4174–4180.
(31) Perdew, J. P.; Burke, K.; Ernzerhof, M. *Phys. Rev. Lett.* **1996**, *77*, 3865–3868.
(32) Eisenmann, B.; Hofmann, A. *Z. Anorg. Allg. Chem.* **1990**, *580*, 151–159.
(33) Hahn, H.; Frank, G.; Klingler, W.; Meyer, A. D.; Stoerger, G. *Z. Anorg. Allg. Chem.* **1953**, *271*, 153–170.
(34) Klee, W.; Schaefer, H. *Z. Naturforsch., B* **1979**, *34B*, 657–661.
(35) Cenzual, K.; Gelato, L. M.; Penzo, M.; Parthe, E. *Z. Kristallogr.* **1990**, *193*, 217–242.

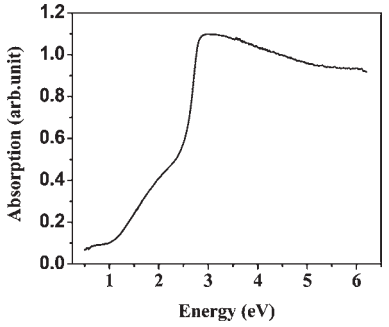

Figure 3. Diffuse reflectance spectrum of $BaGa_4Se_7$.

shortest Ba−Se distance being 3.429(2) A. Thus Ba^{2+} cations have stronger interaction with the $[Ga_4Se_7]^{2-}$ anionic framework in $BaGa_4Se_7$, which will help to stabilize the structure and may be beneficial for the crystal growth and the decrease of defects.

Experimental Band Gap. The UV−visible−NIR diffuse reflectance spectrum of $BaGa_4Se_7$ is shown in Figure 3. A band gap of 2.64 eV and consequently an absorption edge of 0.47 μm could be deduced by the straightforward extrapolation method.[36] The band gap is consistent with the yellow color of the material and is close to that of $AgGaS_2$ (2.70 eV) and higher than that of $ZnGeP_2$ (1.75 eV) and $AgGaSe_2$ (1.8 eV). Band gap has great influence on the laser damage threshold of IR NLO materials. Materials with large band gaps tend to have high laser damage thresholds. Compared with the several practical applicable IR NLO crystals, $BaGa_4Se_7$ possess a relatively large band gap, which suggests that it may have a high laser-induced damage threshold. Besides, the band gap may allow the conventional 1 μm (Nd:YAG) or 1.55 μm (Yb:YAG) laser pumping without the two-photon absorption problem, which has plagued the benchmark IR NLO crystal $ZnGeP_2$.[9]

IR Transmission Spectrum. The IR transmission spectrum of the $BaGa_4Se_7$ crystal is shown in Figure 4. $BaGa_4Se_7$ exhibits high transparency in a broad spectral range up to 0.07 eV (18 μm) in the IR region, covering the important band ranges of 3−5 μm and 8−14 μm of atmospheric transparent windows. Its IR transmission cutoff is longer than that of $AgGaS_2$ (11.5 μm), $ZnGeP_2$ (12.5 μm), and $BaGa_4S_7$ (13.7 μm), which indicates that $BaGa_4Se_7$ may be suitable for a variety of NLO applications in longer wavelength (midfar IR) regions.

Thermal Analysis. The DSC curve is shown in Figure 5. It is evident that $BaGa_4Se_7$ crystal melts congruently at around 968 °C. The congruent-melting behavior is also confirmed by the successful growth of $BaGa_4Se_7$ single crystal from melted $BaGa_4Se_7$ pure powder. In comparison, the melting points are 1088 °C for $BaGa_4S_7$, 998 °C for $AgGaS_2$, 1025 °C for $ZnGeP_2$, and 860 °C for $AgGaSe_2$. The relatively low melting point of $BaGa_4Se_7$ as well as the lower volatility of Se vs S and P will favor the crystal growth by the Bridgman−Stockbarger technique. The congruent-melting behavior of a chalcogenide IR NLO material is valuable because it makes the bulk crystal growth by the Bridgman-Stockbarger technique possible. Bulk single crystals are needed for a thorough

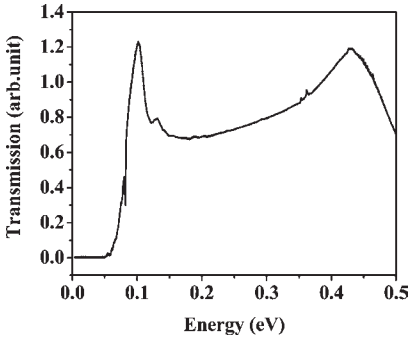

Figure 4. IR Transmission spectrum of $BaGa_4Se_7$ crystal.

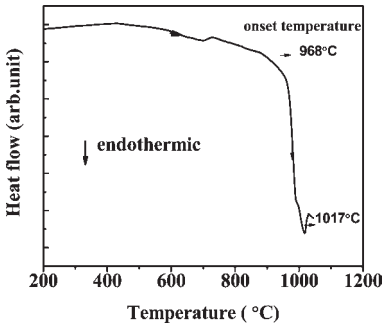

Figure 5. DSC curve of the $BaGa_4Se_7$.

evaluation and practical application of an IR NLO material. The congruent-melting behavior among others makes $BaGa_4Se_7$ a valuable candidate for practically usable IR NLO materials.

Second-Harmonic Generation Measurement. An optical second-harmonic generation (SHG) test was performed on $BaGa_4Se_7$ with the use of a Q-switched Nd:YAG l064 nm laser as the fundamental light. $AgGaS_2$ was used as a reference since it has almost the same absorption edge in the visible region as $BaGa_4Se_7$. Green light (532 nm) was observed, and its intensity was about 2−3 times as large as that of $AgGaS_2$. In comparison, $BaGa_4S_7$ was reported to have a NLO coefficient close to that of $AgGaS_2$.[6,7,20] Thus it can be concluded that $BaGa_4Se_7$ exhibits a SHG effect about 2 times as large as that of $BaGa_4S_7$. Our experimental observation follows the trends in the $AgGaQ_2$ and $LiGaQ_2$ (Q = S, Se) series of compounds, in which the NLO coefficients almost double when the chalcogen changes from S to Se and is consistent with the prediction of the theoretical calculations (see the electronic structure calculation part).

Electronic Structure Calculation. The calculated band structure of the $BaGa_4Se_7$ crystal is plotted along the high symmetry lines in Figure 6. It is shown that the energy band can be divided into three regions; the lower region is located below −11 eV (not displayed), the middle region is the valence band (VB) from about −6 to 0 eV, and the upper one is the conduction band (CB) in which a band of a dispersion spanning about 0.6 eV appears at the bottom of its conduction bands on the Γ point. The calculated direct band gap is 1.76 eV. Further calculations with other kinds of pseudopotentials show that the change of the results is not apparent.

Figure 7 gives the partial density of states (PDOS) projected on the constitutional atoms in $BaGa_4Se_7$, in which several electronic characteristics can be seen: (i)

(36) Schevciw, O.; White, W. B. *Mater. Res. Bull.* **1983**, *18*, 1059–1068.

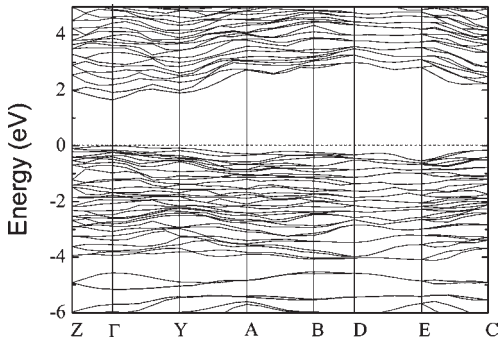

Figure 6. Band structure of $BaGa_4Se_7$ along the lines of high symmetry points in the Brillouin zone. The dash line indicates the VB maximum.

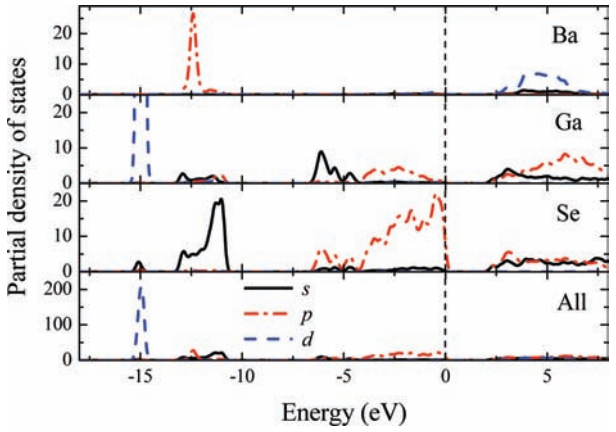

Figure 7. Partial density of states of $BaGa_4Se_7$. The solid, dot-dash, and dash lines are the s, p, and d orbitals, respectively. The broken vertical lines indicate the VB maximum.

The Ba 6s and Ga 3d orbitals are strongly localized in the very deep region of the VB at about −28 eV (not shown) and −15 eV, respectively. Both of the orbitals have no chemical bonding with other atoms. (ii) The VB from −13 to −10 eV are mainly composed of the Ba 5p and Se 4s orbitals, which have some contribution to the Ba−Se bonding. The upper of the valence states from −7 eV show a large hybridization between Ga 4s (and 4p) and Se 4p orbitals, indicating very strong chemical bonds between the Ga and Se atoms, but the valence band maximum is dominated by Se 4p orbitals. (iii) The bottom of CB is mainly composed of the orbitals of Se and Ga atoms, although the Ba 5d orbitals have a little contribution to the higher electronic levels of CB. This means that the $[Ga_4Se_7]^{2-}$ anionic framework directly determines the energy band gap of $BaGa_4Se_7$.

On the basis of the above electronic band structure, the virtual excitation processes under the influence of an incident radiation were simulated, and the refractive indices and second harmonic generation coefficients of $BaGa_4Se_7$ were obtained. It is well-known that the band gap calculated by LDA is usually smaller than the experimental data because of the discontinuity of exchange−correlation energy. In this work, an energy scissors operator[37,38] is adopted to shift all the conduction bands in order to agree with the measured value of the band gap, which is in the good determination of the low-energy structures in the imaginary part of the dielectric functions. Table 3 lists the calculated refractive indices and birefringence at several radiation wavelengths. It is shown that the birefringence Δn is larger than 0.07 as the wavelength is longer than 1 μm, so $BaGa_4Se_7$ is phase-matchable for the second harmonic generation (SHG) in the IR region. Furthermore, we theoretically determined the SHG coefficients of $BaGa_4Se_7$ as follows: d_{11}= 18.2 pm/V, d_{15} = −15.2 pm/V, d_{12} = 5.2 pm/V, d_{13} = −20.6 pm/V, d_{24} = 14.3 pm/V, and d_{33} = −2.2 pm/V. Our calculated results agree with the experimental observation that $BaGa_4Se_7$ exhibits a SHG response 2−3 times that of $AgGaS_2$ (d_{36} = 11 pm/V). Therefore, we are confident that $BaGa_4Se_7$ is a promising candidate for the nonlinear optical applications.

Table 3. Calculated Refractive Indices at Selected Wavelengths for $BaGa_4Se_7$

	1.0 μm	1.5 μm	2.0 μm	$\sim\infty$
n_x	2.87	2.81	2.79	2.77
n_y	2.79	2.74	2.72	2.70
n_z	2.83	2.78	2.77	2.75
Δn ($n_x - n_y$)	0.08	0.07	0.07	0.07

Conclusion

The new compound $BaGa_4Se_7$ has been synthesized for the first time in the A/M/Q (A = alkaline-earth metal; M = In, Ga; Q = S, Se, Te) system. It crystallizes in a NCS space group *Pc*. In the structure $GaSe_4$ tetrahedra are connected to each other by corner-sharing to form a three-dimensional framework with Ba cation in the cavities. Ba is in a "tighter" coordination environment of eight Se compared with that of twelve S in $BaGa_4S_7$. $BaGa_4Se_7$ exhibits a second harmonic generation response at 1 μm that is approximately 2−3 times that of $AgGaS_2$. It has a relatively large band gap (2.64 eV), is transparent up to 18 μm in the mid-IR region, and melts congruently at 968 °C.

$BaGa_4Se_7$ possesses a number of intriguing properties as an IR NLO material: (i) In comparison with the practical usable IR NLO crystal $AgGaS_2$, $BaGa_4Se_7$ has a similar band gap but an approximately doubled NLO effect and a wider IR transparent range up to 18 μm. (ii) Compared with another important IR NLO crystal $ZnGeP_2$, $BaGa_4Se_7$ has a absorption edge of 470 nm in the visible region, which will help to avoid the problem of two-photon absorption of 1 μm laser which has plagued $ZnGeP_2$, and thus make the pumping with the more conventional laser source such as Nd:YAG laser possible. (iii) $BaGa_4Se_7$ exhibits significantly larger NLO coefficient and wider middle IR transparent range than the newly studied IR NLO material $BaGa_4S_7$.

Our preliminary experimental results indicated that $BaGa_4Se_7$ is a new IR NLO material with good overall properties and may find practical application in the future. Further research on the crystal growth of $BaGa_4Se_7$ by the Bridgman−Stockbarger method and a thorough evaluation of its perspective for practical IR NLO application is in progress.

Acknowledgment. This research was supported by the National Basic Research Project of China (2010CB630701). Zheshuai Lin acknowledges the Special Foundation of President of Chinese Academy of Sciences.

Supporting Information Available: Crystallographic files in CIF format for $BaGa_4Se_7$. This material is available free of charge via the Internet at http://pubs.acs.org.

(37) Godby, R. W.; Schluter, M.; Sham, L. J. *Phys. Rev. B* **1988**, *37*, 10159–10175.
(38) Wang, C. S.; Klein, B. M. *Phys. Rev. B* **1981**, *24*, 3417–3429.